

# Effect of bacterial nanocellulose on the fresh and hardened states of oil well

Juan Cruz Barría, Analía Vazquez, Jean-Michel Pereira, Diego Manzanal

▶ **To cite this version:**

Juan Cruz Barría, Analía Vazquez, Jean-Michel Pereira, Diego Manzanal. Effect of bacterial nanocellulose on the fresh and hardened states of oil well. Journal of Petroleum Science and Engineering, 2021, 199, pp.108259. 10.1016/j.petrol.2020.108259 . hal-03169623

**HAL Id: hal-03169623**

**https://enpc.hal.science/hal-03169623**

Submitted on 17 Mar 2021

**HAL** is a multi-disciplinary open access archive for the deposit and dissemination of scientific research documents, whether they are published or not. The documents may come from teaching and research institutions in France or abroad, or from public or private research centers.

L'archive ouverte pluridisciplinaire **HAL**, est destinée au dépôt et à la diffusion de documents scientifiques de niveau recherche, publiés ou non, émanant des établissements d'enseignement et de recherche français ou étrangers, des laboratoires publics ou privés.

Revised manuscript with no changes marked

# Effect of bacterial nanocellulose on the fresh and hardened states of oil well cement

**Juan Cruz Barría[1,3], Analía Vazquez[2], Jean-Michel Pereira[3], Diego Manzanal[1,4,5 *]**

(1) *Universidad Nacional de la Patagonia, Facultad de Ingeniería, Dpto. Ingeniería Civil, - CONICET, RP Nº1 km4, Ciudad Universitaria, 9005, Comodoro Rivadavia, Argentina*

(2) *Universidad de Buenos Aires (UBA), Facultad de Ingeniería, LAME, Av. Las Heras 2214, 1426, Buenos Aires, Argentina, Av. Las Heras 2214, Buenos Aires, Argentina*

(3) *Navier, Ecole des Ponts, Univ Gustave Eiffel, CNRS, Marne-la-Vallée, France.*

(4) *Instituto de Tecnología y Ciencias de la Ingeniería (INTECIN), Universidad de Buenos Aires (UBA), CONICET, Facultad de Ingeniería, Av. Las Heras 2214, 1426, Buenos Aires, Argentina.*

(5) *ETS de Ingenieros de Caminos, Canales y Puertos, Universidad Politécnica de Madrid, c/ Prof. Aranguren 3, Ciudad Universitaria, 28040, Madrid, Spain (Current).*

**corresponding author: d.manzanal@upm.es*

## Abstract

The evaluation of oil well cement additives is determined by the influence on the rheological and mechanical properties of the slurry. The use of nanoadditives for cement, such as bacterial nanocellulose (BNC), has been increasing in recent years due to their high tensile strength, high Young's modulus, and thermal resistance. However, the influence of BNC addition on the mechanical properties of the cement is not widely studied. The purpose of this work is to understand the effects caused by the addition of BNC in class G cement during the fresh and hardened states. Free fluid and high-pressure consistometry tests have been carried out in the fresh state. In the hardened state, dynamic thermomechanical analyses (DMA) and uniaxial compressive strength (UCS) tests have been performed. Additionally, thermogravimetric analysis (TGA) was carried out to determine the calcium hydroxide content and the hydration degree (DOH). Results indicate that BNC modifies the slurry behavior by reducing the free fluid content and by incrementing consistency. Moreover, the calcium hydroxide content and DOH increase with the addition of BNC. The mechanical properties of BNC-cement samples are increased in terms of storage modulus and mechanical strength. These properties can improve the performance of cement used in cementing operations.

## Keywords

Bacterial Nanocellulose – Cementing – Mechanical Performance – Thermal Analysis

## 1. Introduction

Oil well cementing is a complex procedure in wellbore operations. The cement must ensure the oil well integrity and prevent links between formations (Al Ramadan et al., 2019; Kiran et al., 2017). The slurry used differs from each particularly well condition, changing its additives and quantities as needed. This cement mixture must meet a series of requirements according to Standards, and it will be subjected to several stress loadings throughout its life span. Different problems arise during these stages, but the low tensile strength and cracks propagation of the set cement (Banthia and Nandakumar, 2003) and its resistance to temperature are essential properties to be optimized, as well as.

Recently, there has been a growing interest in nanocellulose (Charreau et al., 2012). Nanocellulose has a background in reducing micro-cracking (Hisseine et al., 2019, 2018). Its addition to cement is very likely to induce an increment in tensile strength and prevent the propagation of cracks caused by external loads. There are three types of nanocellulose according to how is production; microfibrillated nanocellulose (MFC), nanocrystalline cellulose (NCC), and bacterial nanocellulose (BNC).

Bacterial nanocellulose is an environmentally friendly material (Muhd Julkapli and Bagheri, 2017) produced by several bacteria types in different culture media. In particular, *Gluconacetobacter xylinus* bacteria is one of the primary microbial producers of this material, and its research is still ongoing (Keshk, 2014), with essential advances about bacterial cultivation (Mikkelsen et al., 2009) (Vazquez et al., 2013). New studies on the cost-effectiveness of culture media are making its production a significant subject of interest for industrial applications (Jozala et al., 2016).

Recently, there has been new production of bacterial nanocellulose utilizing residues from the wine industry and using steep corn liquor, which demonstrated a four-time higher yield of this product in an inexpensive fermentation medium (Cerrutti et al., 2016). This increase in quantity becomes significant after 21 days of incubation, and also its structure is more

compact and dense because it generates a more substantial number of branches that intertwine with each other (Sheykhnazari et al., 2011). These denser nanocellulose fibers are obtained with nanometric widths in the ranges of 18 to 57 nm and micrometers in length, thus obtaining a high specific surface area material.

Several authors have proved that nanocellulose improves the mechanical, thermal, and microstructural properties of cement-based compounds (Sun et al., 2016; Vazquez et al., 2013, Barria et al., 2018, 2019, 2020a,b). Mainly, studies focused on the research of MFC, and NCC. The improved properties were compressive strength, thermal performance, degree of hydration, viscosity and water retention of cement (de Paula et al., 2014; Gómez Hoyos et al., 2013; Mejdoub et al., 2017; Savastano et al., 2005).

However, there are few studies on the Bacterial nanocellulose (BNC) (Mohammadkazemi et al., 2017, 2015, Barria et al. 2018, 2019). Recently, BNC has been used to modify properties of the drilling fluids, enhanced oil recovery (EOR), and oil well cementing (Ramasamy and Amanullah, 2020). BNC is estimated to have a similar effect of that MFC and NCC on cement. The use of BNC in cement mortars shows an improvement in flexural and compressive strength (Akhlaghi et al., 2020).

Therefore, the study of bacterial nanocellulose as an additive for oil well cement class G is an exciting alternative to improve its performance in petroleum engineering applications. The purpose of this work is to understand the changes due to the use of bacterial nanocellulose (BNC) as an additive in class G oil-well cement during fresh and hardened states. We examine the rheological behavior of an oil well cement slurry modified with different percentages of BNC by performing free fluid and consistometry tests. The thermal and mechanical behavior of cement class G with different BNC content is analyzed by dynamic mechanical analysis (DMA) and unconfined compression strength (UCS) test. In addition, the degree of hydration (DOH) of the cement paste with the addition of BNC performing a thermogravimetric analysis (TGA) is investigated.

## 2. Materials

The cement used in this study was a Class G Portland Cement provided by PCR S.A. (Petroquímica Comodoro Rivadavia S.A., Argentina). It is made with clinker and calcium sulfate of high sulfate resistance grade to satisfy the chemical requirements of the American Petroleum Institute (API) Specification 10A for cement (API Specification 10A, 2019): $C_3S$ 52.8%, $C_3A$ 1.6%, $C_2S$ 21.1% and $C_4AF$ 15.5%. The chemical composition was obtained by X-ray fluorescence (XRF) and is given in Table 1. The XRF system consists of an X-ray generator tube, collimators, crystals, and beam detectors. The excitation of the atoms from the X-rays emits radiation that is detected by the equipment, thus quantifying the chemical composition of the cement.

Bacterial nanocellulose (BNC) is a polymer derived from cellulose obtained from the aerobic fermentation of bacteria of the genus *Gluconacetobacter* as the primary extracellular metabolite (Charreau et al., 2012). It was provided by a spinoff of ITPN-CONICET (Nanocellu-Ar) in the form of a membrane in sealed jars (Cerrutti et al., 2016). The nanocellulose has a repetitive molecular structure composed of a linear backbone of β(1-4)-linked d-glucose units (Cerrutti et al., 2016; Vázquez and Pique, 2017). The difference between BNC and other polymers relies on the fact that it does not possess free macromolecules; it is a membrane formed by micrometric fibers of nanometric thickness. Fig. 1 shows the bacteria and the interconnected nanocellulose network. These membranes contain approximately 98% water and 2% BNC.

Deionized water and a superplasticizer were used in the mixture. The superplasticizer (SP) additive used was the ADVA 175 LN High-Performance Water-Reducing Admixture with a light-yellow liquid appearance and a density of 1.06 g/cm$^3$. It is an additive with characteristics like those of a polycarboxylate (Puertas et al., 2005).

## 3. Sample preparations and experimental method

### 3.1 Sample preparation

The slurry samples were mixed according to API specifications. A high-speed mixer with an API standard blade type was used (API Specification 10A, 2019). The mixing procedure consisted of 15 seconds of a rotation speed of 4.000 ± 200 rpm, and then, 35 seconds of 12.000 ± 500 rpm. The cement was passed through an ASTM No. 20 sieve. Each sample was prepared with 792 ± 0.5 g of cement and 349 ± 0.5 g of distiller water at a temperature of 23 ± 1 °C.

BNC membranes were wet-grinded to obtain the BNC additive. Then, the BNC-distilled water mixture was conditioned in a 6.5 L Arcano ultrasonic bath with a frequency of 40.000 Hz for 30 minutes. This procedure breaks up the nanocellulose agglomerates fibers (Fig. 2). The use of the ultrasound technique improves the mechanical properties of the mixture by dispersing the nanocellulose and generating a more homogeneous paste (Barbash et al., 2016). The BNC proportion was determined by weighing three representative samples from the additive before and after placing the samples inside an oven for 24 hours. Free water was evaporated, and the average quantity of BNC obtained was approximately 0.46%. Afterward, the BNC-distilled water mixture was placed in the high-speed mixer according to the percentage of BNC addition. Additional distiller water with SP was added to obtain a W/C ratio of 0.44 by weight.

The addition of BNC can improve specific properties of the cement, such as an increase in the degree of hydration (Cao et al., 2015), an increase in mechanical strength (Sun et al., 2017), and this may reduce porosity. However, the addition also generates changes in the rheological properties of the slurry (Hoyos et al., 2019). Since the previous studies contemplate the changes produced by the use of different types of nanofibers, this work aims to perform comprehensive research regarding the effects made only by bacterial nanocellulose in the fresh and hardened states of class G cement.

Experiments were conducted on samples with ordinary Portland cement (PC) and cement modified with percentages of BNC of 0.05, 0.10, 0.15, and 0.20 by weight of cement (BWOC). Table 2 shows the details of each cement mixture.

### 3.2 Free fluid test

The free fluid or free water content is the volume of fluid that separates from the cement slurry once the slurry remains at rest. Slurry samples of PC and modified PC with BNC were performed in accordance with the API Standard 10A (API Specification 10A, 2019). After the high-speed mixing (section 3.1), the slurry samples were placed in an atmospheric consistometer. The atmospheric consistometer consists of a rotating cylindrical slurry container equipped with a stationary pallet system. The rotational speed is 150 ± 15 RPM. The vessel was kept at a controlled temperature of 27 ± 2 °C in an oil bath. After stirring the slurry for 20 minutes ± 30 seconds in the atmospheric consistometer, 760 ± 5 g of slurry were transferred directly to a 0.5 L Erlenmeyer flask within 1 minute of completion of mixing. The flask was kept on an anti-vibration surface for 2 hours, and the excess liquid at the top was removed and measured with a pipette. The percentage of free liquid was calculated using the following formula:

$$\varphi = \frac{V_{FF} \cdot \rho}{m_s} \cdot 100 \qquad (1)$$

Where φ is the volume fraction of free fluid expressed as a percentage, $V_{FF}$ is the volume collected with the pipette, $m_s$ is the mass of the slurry in grams and ρ is the density of the slurry in g/cm$^3$ which is associated with the cement density.

The cement density was obtained following the IRAM 1624 Standard. The cement (64 g) was placed into a Le Chatelier flask containing 0.5 cm$^3$ of kerosene at room temperature of 20 ± 2 °C and relative humidity 50%. After removing the retained air, the final reading was measured after 150 ± 30 min. The cement density obtained was 3.18 ± 0.01 g/cm$^3$. The slurry density associated is 1.91 g/cm$^3$.

### 3.3 High-pressure Consistometer

Cementing a wellbore requires a cement slurry capable of maintaining an adequate state of pumpability under downhole conditions over a specific range of time. Thickening time was determined with a high-temperature and high-pressure consistometer following the API Specification 10A (API Specification 10A, 2019). The consistency of the slurry over time is measured in Bearden units ($B_C$).

The cement slurry (section 3.1) was poured into a standardized container and stirred at a constant speed. A ramp of temperature and pressure over time was applied to the system until Bearden unit of consistency reached 100 Bc for a specific time. This time is known as the thickening time of cement. The consistency should be less than 30Bc between 15 and 30 minutes after the beginning of the test to ensure adequate initial consistency. In the field, the time to 100 Bearden units represents the amount of time cement remains pumpable under well conditions. Bearden units are dimensionless, cannot be converted to any viscosity unit, and can only be determined by the high pressure and temperature consistometer.

### 3.4 Thermogravimetric analysis

Cement is a porous multi-phasic material whose main components are hydrated calcium silicate, calcium hydroxide, and calcium aluminate hydrate. When comparing two different cement types of the same age, the calculation of the hydration degree is useful. It estimates the amount of anhydrous cement that has reacted with water to form the cement hydrates. The quantity of calcium hydroxide and the hydration degree can be obtained from the thermogravimetric analysis.

The determination of non-evaporable water, calcium hydroxide (CH), and hydration degree (DOH) was carried out by the technique of thermogravimetric analysis. The TGA-50 Shimadzu equipment consists of a precision balance, where the sample was placed inside a platinum tray in a nitrogen atmosphere and a furnace that was programmed to increase the temperature from 25 to 800 °C at a constant heating rate of 10 °C/min with a constant temperature hold at 140 °C for 15 min. Finally, the tests ended when the temperature reached 800 °C and was maintained for 1 minute.

A total of five samples were crushed and analyzed in the TGA, one for each percentage of nanocellulose (0%; 0.05%; 0.1%; 0.15%; 0.20% BWOC). Each sample had an approximate weight of 0.008 g. The powdered material was dried at 110 °C for 24 hours to remove free water (Palou et al., 2014).

The portlandite content is obtained with the technique proposed by (Sun et al., 2016):

$$\mathrm{CH}[\%] = \frac{74.09}{18.01} \cdot \mathrm{WL}_{\mathrm{CH}}[\%] \quad (2)$$

Where $WL_{CH}$ is the percentage of weight loss during the test. The degree of hydration (DOH) is determined by relating chemically bound water (CBW) burned to the maximum CBW burned for cement. The maximum CBW value in ordinary cement is 0.23 g of bound water per g of a burned sample (Pane and Hansen, 2005). Therefore, the DOH of the samples studied can be calculated as the weight of CBW burned between 140 and 800 °C:

$$\mathrm{DOH}[\%] = \frac{(\mathrm{w}_{140} - \mathrm{w}_{800})}{0.23 \cdot \mathrm{w}_{800}} \cdot 100 \quad (3)$$

### 3.5 Dynamic mechanical analysis

Cement undergoes temperature variations during its life span when it is used as annular protection for the wellbore. Cement is mechanically affected when a temperature gradient is applied to it.

In order to evaluate the thermo-mechanical properties of cement, a dynamic mechanical analysis (DMA) was performed. DMA measures these properties as a function of time and temperature while the material is subjected to a periodic oscillatory force (García, 2012). In this case, oscillatory bending stress. The storage modulus (E′) is the stiffness of the material and represents the capacity of the material to store the applied energy. The loss modulus (E″) is the capacity of the material to dissipate the applied energy and is also related to the viscous response of the material (Jawaid et al., 2015). The vector composition between the storage modulus and loss modulus is the complex modulus (shear modulus) (E*). The angle formed by these vectors is the mechanical damping factor of the material (δ) (Saba and Tahir, 2016). A material that can store a large amount of applied energy will have a small angle δ (high elasticity).

The dynamic mechanical analysis was performed with a Perkin-Elmer DMA 8000 instrument using the three-point bending mode. The deformation imposed on each pulse was 0.001 mm, with a pulse frequency of 1 Hz. The test began at room temperature and increased until 200 °C with a constant rate of 2 °C/min. For each pulse, the storage modulus was measured. A total of 20 samples of 3 mm × 9 mm × 30 mm were tested, four for each nanocellulose percentage (0%; 0.05%; 0.1%; 0.15%; 0.20% BWOC).

3.6 Unconfined compressive strength (UCS)

After mixing according to Section 3.1, the slurry was poured into standard cubic molds of 5 cm per side following the API specifications (ASTM International, 1999) for the subsequent compressive strength tests. The molds were placed in the curing chamber at a temperature of 20 ± 1 °C, and after 24 hours inside the molds, the specimens were removed and put back inside the chamber. Once the curing time had passed, the axial compression test was performed with planar metalheads at a velocity rate of 72 ± 7 kN/min (Fig. 3).

The tests were performed using bacterial nanocellulose with percentages of 0.05%, 0.1%, 0.15%, and 0.2%, with adequate percentages of SP to obtain workability, and were cured for 7 and 28 days in order to understand the compressive strength evolution over time. The results are obtained from an average of 3 samples for each percentage of BNC used. The absolute variation from the average was considered for the analysis.

A flow chart of the testing methodology is shown in Fig. 4.

## Results and discussion

4.1 Effect of BNC on cement slurries: free fluid content, consistency and thickening time

Cementing a wellbore requires a slurry capable of maintaining an adequate state of flowability under downhole conditions over a specific range of time. Moreover, once the oil well-cementing procedure is completed, the cement slurry requires to keep the cement solids in suspension in the early and middle hydration periods. The effect of the BNC and SP additions on the rheological behavior of cement slurry is analyzed through free fluid and consistometer test.

Fig. 5 shows the evolution of the free fluid content [%] of Portland cement (PC) and PC + 0.05% BNC slurries with the addition of SP. PC slurry shows 1.89% of free fluid content measured by equation 1. The free fluid of PC + 0.10% SP and PC + 0.30% SP slurries is reduced by 5% and 36%, respectively. The results show a clear trend of decreasing the free fluid content of the PC slurries with the increment of SP addition. However, large amounts of these additions will allow more air bubbles to enter into the cement paste, thus incrementing cement porosity and decreasing long-term mechanical properties and durability. The reduction in the free fluid with SP has been already studied, and the stabilization in the slurry occurs because of the content of polycarboxylates which chemically modifies the behavior of the cement in the fresh state (Moumin and Plank, 2017).

A similar trend is observed in PC slurries with the addition of 0.05% of BNC. The free fluid is significantly reduced by the addition of the BNC for a given SP value, as is shown in Fig. 5. For the addition of 0.10% SP, the reduction of free fluid observed in PC + 0.05%BNC slurry is 76% in comparison with the PC slurry. This gap decreases as the amount of SP increases. For instance, the free fluid content of PC + 0.05%BNC is reduced 52% in comparison with the PC slurry for the addition of 0.35%SP. Thereby, the limitations and correct doses of SP are critical.

Results in the modified cement slurries with BNC might be explained by the water holding capacity within the mixture of the BNC (Gómez Hoyos et al., 2013). Water is adhered to the surface of BNC fibers and thickens the mixture (Balea et al., 2019). We can see in previous studies that no water can be extracted if the quantity of nanocellulose applied is excessive (Hoyos et al., 2019).

Results show that when using both nanocellulose and superplasticizer, the slurry stability increases, which helps to prevent a fluid breakout. This effect of fluid breakout is usually accompanied by longitudinal fluid channeling, which allows gas migration (Bonett and Pafitis, 1996; Nelson, 1990; Salehi et al., 2016), and by reducing this effect on the modified cement, an extension of its durability can be achieved.

During wellbore cementing operations, if the cement slurry maintains a liquid state for a short time, the constant pumping will damage the cementitious structure generated by its initial setting. On the other hand, if the liquid state is maintained for a long time, it may delay the commissioning of the well. With the addition of BNC to the cement slurry, an increase in the yield stress is observed (Hoyos et al., 2019; Sun et al., 2016). However, there is no clear understanding of the dynamic behavior of the modified slurry concerning temperature changes. In order to observe the rheological behavior under temperature and pressure of the cement modified with BNC, consistometry tests were performed to PC and cement with the addition of 0.05% BNC. The initial consistency and the thickening time were evaluated for different percentages of SP to obtain slurry workability similar to PC. The results are shown in Table 3.

Three different tests are shown in Fig. 6; tests 1 (Portland cement), 5 and test 6 (Cement + 0.05% BNC). Consistencies are shown along the Y-axis versus time along the X-axis. Test 1 describes the normal curve for unmodified class G oil-well cement. In the cases of BNC-modified slurries with additions of SP less than 0.3%, samples quickly become very viscous, reducing workability with consistency values above the tolerable value (30 Bc). This behavior is different from other polymers, where it has been found that a natural cellulose polymer increases thickening time (Abbas et al., 2013). The difference with their experiment is that hydroxypropylmethylcellulose acted as a retarding agent to cement setting, allowing the slurry to remain in a liquid state. In our case, BNC acts like a water retainer, removing water used for workability and adsorbing it. This effect reduces the initial cement hydration, but at the same time, it considerably increases consistency in Bearden units, reducing thickening time. BNC has a width range between 18 to 57 nm and micrometers in length (Cerrutti et al., 2016), which can lead to a specific surface area variance between 150 and 250 $m^2/g$ (Li et al., 2017). Hence, the water employed in cement workability is now reduced to wet this new surface. The addition of 0.1% of BNC considerably increases the yield stress (Hoyos et al., 2019), while an increment of 0.4% leads to a cement paste that is impossible to flow.

The consistency of BNC-modified slurries with additions of SP of 0.35% approximates to the PC behavior. Despite this behavior being erratic through time, the final thickening time is similar to the reference cement. However, BNC-modified slurries with additions of SP of 0.35% have an initial consistency higher than the PC slurry, due to the higher initial yield stress. On the other hand, the modified samples with additions of SP of 0.4% present a smaller initial consistency, and the thickening time is 25 min longer than the PC and modified samples with additions of SP of 0.35%. This effect is caused by the SP, which makes the mixture more fluid and needs more time to thicken. Larger quantities of SP reduce the probability of the hydration reaction and the precipitation of solid cement particles during the first hours, allowing the sample to remain in a liquid state for longer.

4.2 Effect of BNC on the degree of hydration

TGA and DrTGA results are shown in Fig. 7 and Fig. 8, respectively. The content of each material phase was calculated by drawing three tangential lines on the TGA graph, and the vertical difference of mass percentage between the intersections is considered the decomposition of the material (Marsh and Day, 1988; Sun et al., 2016; Wild and Khatib, 1997). The continuous loss of mass on the graph is due to the dehydration of CSH and other compounds that starts at 105 °C and continue until the end of the test (DeJong and Ulm, 2007; Palou et al., 2014). The drop in mass between 420 and 480 °C is due to the portlandite decomposition into $Ca^{2+}$ ions and $2HO^-$ from which CaO and $H_2O\uparrow$ are produced (De Weerdt et al., 2011). We also can see a small drop between 600 and 650 °C, which is the decomposition of calcite. But considering that this cement was kept under alkaline distilled water with negligible carbonation in the samples during 28 days (Tuutti, 1982) and given the fact that the samples were dried in an oven at 110 °C during 24 hours, we can assume that this calcite is, in fact, portlandite that was carbonated during drying and formed into calcite due to accelerated carbonation in the oven, increasing the $CO_2$ uptake (Liu et al., 2001). The shape of the curves is similar for those samples with and without additions, and they do not show new products due to BNC or SP addition (Ma et al., 2011). The curves of 0.05% and 0.15% content of BNC cannot be distinguished.

Portlandite content increases with the BNC content, as we can see in Table 4. The BNC water retainer effect generates an additional source of water, which is enhancing the generation of hydration products (Gómez Hoyos et al., 2013; Hisseine et al., 2019). On the other hand, the degree of hydration (DOH) is higher in all percentages of BNC compared to PC. Similar behavior can be found in the literature (Sun et al., 2016). The DOH values are underestimated because they were obtained at 800ºC instead of 1100ºC. However, it shows a trend in all the samples analysed.

Cement hydration and development of the microstructure over time are complex processes whose study is not the objective of this work. However, an explanation of the increment in DOH and CH content is necessary. The surface free energy (SFE) is an indicator that can characterize if a surface is more or less hydrophobic. The sum of the dispersive and polar components gives the SFE. According to the literature, dispersive surface energy can increase up to 138% by adding BNC to the cement sample (Mohammadkazemi et al., 2017). This causes more hydration reactions due to the increased amount of water on the surfaces of the cement microstructure. Therefore, the increase in SFE explains the increase in portlandite (CH) and DOH. Calorimetry tests on nanocellulose materials have shown an increase in heat release (Cao et al., 2015; Lee et al., 2019), thus obtaining a higher hydration degree. However, initially, it acts as a retarder for cement (Cao et al., 2016; Fu et al., 2017). Hisseine (Hisseine et al., 2019) suggested that the heat increment during the calorimetry test is associated with the alkaline hydrolysis of cellulose, which promotes cement hydration. Furthermore, cellulose filaments tend to release water during hydration (Hisseine et al., 2018). In our experiments, BNC is in line with the nanocellulose effects on cement mentioned in the literature, incrementing the hydration degree and portlandite content.

### 4.3 Effect of BNC on the mechanical performance: dynamic mechanical analysis and unconfined compressive strength

The stiffness of the material is calculated from the deformation under load. The storage modulus E' is a function of the elastic properties of the samples, and it is analogous to the static modulus of elasticity or Young's Modulus.

The values obtained by the DMA results of the storage modulus are observed on a logarithmic scale in Fig. 9. This modulus is reduced by increasing temperature. Samples with 0.15% and 0.20% of BNC maintain higher magnitudes than PC from 20°C to 200°C, while 0.05% of BNC has lower values throughout the test. BNC can maintain properties while the temperature is rising in the medium, which is traceable to its thermal stability up to 350 °C (Hoyos et al., 2019). The reduction of the stiffness (E' values) during the first step until 110 °C is due to dehydration of the free adsorbed water and some interlayered water (Sereda et al., 1966) which speed up the start to micro-cracking of the sample (Evans and Marathe, 1968).

In Fig. 10, we normalized the storage moduli to their initial values. The normalized storage modulus is obtained by dividing the module measured at a certain temperature ($T_i$) over its initial value ($T_0$) for each tested sample. An important drop is observed between 110 and 140 °C, where cement samples lose between 80% and 50% of their storage modulus. This drop can be explained due to water evaporation from the samples and to CSH dehydration, starting at approximately 110 °C (Foray-thevenin et al., 2006). The dehydration begins to degrade the properties of the cementitious matrix because the water acts as a stabilizer of the CSH structure. Here, cement with 0.15% of BNC has a better performance than PC and cement modified with 0.05% or 0.20% of BNC. These samples are the most stable mixtures, due to that quantity is better distributed in the sample. BNC acts like water molecules and pulls apart the CSH interlayer. For the other samples, a more rapid collapse of the CSH structure with dehydration occurs. More sliding sites, increment in the internal friction, and a faster reduction of the elasticity consequently decreases quicker the value of E with temperature (Alizadeh et al., 2011). At 130°C, PC shows a lost 70% of its modulus, while samples with 0.15% of BNC only lost 30%.

On the other hand, the storage modulus of the 0.05% BNC sample is smaller than the PC samples for most of the test, except between 130 and 160 °C. However, the normalized module graph shows better behavior after 120°C. This means that this small addition of BNC changes the thermal properties but does not change the bending strength.

In Fig. 11, temperature provokes a significant impact on the PC sample, inducing higher tan δ, which represents the material resistance to be deformed by temperature. This effect starts to be detected at 150 °C and until 200 °C. On the other hand, cement with a higher percentage of BNC (0.15% and 0.20%) has not been affected as the previous one. It has maintained a lower loss modulus factor (85% less than PC at 200 °C), except for the percentage of 0.05%, where the reduction is 50%. Considering the analysis of nanostructure performed by Alizadeh et al. (Alizadeh et al., 2011), the behavior of tan δ of PC and 0.05% of BNC is different from 0.15 and 0.20 % BNC. This can be related to the different microstructure generated due to the formation of aggregates of BNC in the mixture with PC. Alizadeh et al. related the higher tan δ value to higher E¨, and sliding frictional effects that occur when water is evaporated from adsorbed water because water restrains the CSH sheets. The decrease of tan δ or damping effect is the consequence of higher rigidity of the nanostructure. This is the result of a higher bridging of the CSH sheets due to the increases in the number of strong bonds between SI and O or Si-O_Ca. These bonds are due to the dehydration of water interlayer of CSH, which is higher for a higher content of BNC.

As seen before on the microstructure of cement, PC has the lowest hydration degree of the samples. The lower quantities and shorter length chains of CH are making this cement more susceptible to creep (Pourbeik et al., 2013), while samples with higher hydration degrees are withstanding the oscillatory loading. On the other hand, cement samples under bending mode are very dependent on the material tensile strength. Fatigue crack propagation depends on the applied stress, the initial crack size, and the material toughness to fracture. As the applied stresses are the same (bending load and temperature rate changes), the samples reinforced with BNC induce two types of changes. The first

change occurs on the pre-testing cracking size (tensile strength improvement) and the second one on the fracture toughness (hydration improvement). These changes explain the behavior of the samples at 200°C, where all modified samples with BNC have shown higher storage modulus than PC, except with 0.05%.

Previous studies have worked with other polymers and also found that fibers add more flexural strength in cement (Jamshidi and Karimi, 2009; Parveen et al., 2017). Our results show this trend on flexural strength, and now it shows improvement under thermal stresses. Samples of 0.15 and 0.20% BNC increase the properties at room temperature and up to 200°C

The tensile strength of cement samples is around 10% of the unconfined compressive strength for Portland cement. The addition of BNC increases the tensile stress reinforcing the samples and increasing compressive strength (Parveen et al., 2017).

The compressive strength of BNC-cement mixtures was determined for samples cured in a water bath at 20 °C during 7 and 28 days.

Fig. 12 shows the normalized compressive strength of cement as a function of BNC percentages cured for 7 and 28 days. The strength values ($\Delta$) are normalized to the strength value obtained after 7 days of curing in PC cement ($\Delta_0$). The error bars show the absolute variation obtained in the tests. The unconfined compressive strength of PC, and the mixtures PC + 0.05%, 0.10%, 0.15% and 0.20% BNC for different curing times is presented in Fig. 13. The errors in the PC and 0.05% samples are very small in Fig 12, so their error bar is not visible in the graph. To plot Figure 13, only the average values of the results were used.

The results show an enhancement in strength for cement samples with the addition of BNC. However, PC + 0.15% BNC and PC + 0.20% BNC samples at 7 days shown a decrease in the strength influenced by the segregation in the mixture due to the SP (Xiaofeng et al., 1990). It is known that other types of nanocellulose increases compressive strength as well (Hisseine et al., 2019; Lee et al., 2019; Mejdoub et al., 2017). The increase in tensile stress (Cao et al., 2015), compressive strength, and hydration degree support the use of BNC as

a long-term reinforcement. The hydrophilic characteristic of BNC to avoid faster water loss during cement hydration is preventing the propagation of thermally induced cracking (Balea et al., 2019). By decreasing these cracks, the probability of failure through them for the same stress is decreased (Banthia and Nandakumar, 2003; Lee et al., 2019), allowing the bulk sample to withstand more loading.

The strength tends to increase with the percentage of nanocellulose. A small increment in BNC (0.05%) produces an important increment in compressive strength, both at 7 days and at 28 days. The addition of 0.05% BNC increases by 18% and 20% the strength in comparison with cement sample (PC) cured at 7 days and 28 days, respectively. Other authors also obtained a significant rise in strength for small percentages of nanocellulose addition (Hisseine et al., 2019; Sun et al., 2016). The results are encouraging the use of BNC in future admixtures due to its low amount of incorporation and low change in the viscosity.

## 5. Conclusions

An experimental study regarding the effects produced by the addition of bacterial nanocellulose (BNC) between 0.05% to 0.20% BWOC to cement was carried out. Free fluid tests, high-pressure consistometry tests, thermogravimetric analysis, thermomechanical analysis, and uniaxial compressive strength tests were performed.

Results indicate that the addition of BNC between 0.05% to 0.20% BWOC produces an important decrease in the amount of free fluid.

The addition of BNC reduces the thickening time of cement slurry, and a dispersive agent is needed to maintain the fluidity of the mixture. Nevertheless, more significant amounts of dispersant increase the thickening time for the same amount of nanocellulose.

The thermogravimetric analysis shows an increment in hydration products and hydration degree as the percentage of bacterial nanocellulose increases due to its hydrophilic properties.

The dynamic mechanical analysis shows an improvement in the thermoelastic behavior of cement pastes by using large percentages of BNC, mainly by its thermal stability and its tensile reinforcement.

The use of BNC in cement has shown an increment in strength development at 7 and 28 days. All the mixtures using bacterial nanocellulose have increased the compressive strength development over time.

In summary, the 0.05% additions BWOC of bacterial nanocellulose have shown good performance for tests with fresh and hardened cement samples. In fresh cement samples, the workability is achieved with small amounts of superplasticizer, and the free fluid is suitable to be used in the consistometer. The mechanical properties obtained during thermo-mechanical tests (DMA) are similar to ordinary cement, but a significant increment in compressive strength is observed. The results are beneficial up to 0.20% BWOC of BNC used, although a more considerable amount of superplasticizer is needed to maintain the fresh samples' fluidity.

The addition of bacterial nanocellulose between 0.05% to 0.20% BWOC improves the mechanical properties of the cement due to its tensile strength and crack inhibition. Another reason for this might be the increase in hydration degree, which generates more CSH and CH that increase its strength. The water retention of BNC increases its initial consistency. However, it produces a considerable decrease in its free fluid content, which enhances its hydration. Further analysis of microstructure is underway to characterize the modified cement.

Bacterial nanocellulose proves to be an inexpensive, renewable, and high-strength material that can be used as an additive to oil well cement. These characteristics can benefit the cement used during well-cementing operations. Due to its low free fluid content, the probability of fluid migration in the well may be reduced. The increase in thermal and mechanical strength can improve the performance of the cement sheath surrounding the casing, having a better behavior when supporting the stresses generated by temperature gradients or induced seismic activity during water or $CO_2$ injection scenarios.

## Acknowledgment

The first author gratefully acknowledges the fellowship granted by CONICET (National Scientific and Technical Research Council – Argentina). The authors also acknowledged the financials support of "*Universidad Nacional de la Patagonia San Juan Bosco"* (Project UNPSJB PI1614 – 80020190200006IP, Resol R/9Nº207-2020 CRD1365 FI004/17) and the Agency of Scientific and Technological Promotion (Agencia Nacional de Promoción Científica y Tecnológica) from Ministry of Science and Technology of Argentine Republic. (Projects PICT 2016-4543). The authors express their gratitude to Petroquímica Comodoro Rivadavia S.A. and its technical staff for helping with the performed tests.

## Abbreviations

| | |
|---|---|
| *API:* | *American Petroleum Institute* |
| *BNC:* | *Bacterial nanocellulose* |
| *BWOC:* | *By weight of cement* |
| *$C_3S$:* | *Alite* |
| *$C_3A$:* | *Calcium aluminate* |
| *$C_2S$:* | *Belite* |
| *$C_4AF$:* | *Calcium alumino-ferrite* |
| *CH:* | *Calcium hydroxide* |
| *CSH:* | *Calcium silicate hydrate* |
| *CBW:* | *Chemical bound water* |
| *DMA:* | *Dynamic mechanical analysis* |
| *DOH:* | *Degree of hidration* |
| *DrTGA:* | *Derivative hermogravimetric analysis* |
| *EOR:* | *Enhanced oil recovery* |
| *MFC:* | *Microfibrillated nanocellulose* |
| *NCC:* | *Nanocrystalline cellulose* |
| *PC:* | *Portland Cement* |
| *SP:* | *Superplasticizer* |
| *TGA:* | *Thermogravimetric analysis* |
| *UCS:* | *Uniaxial compressive strength* |
| *W/C:* | *Water to cement ratio* |
| *XRF:* | *X-ray fluorescence* |

## Nomenclature

| | |
|---|---|
| $\delta$: | *Mechanical damping factor [ ]* |
| $\Delta_0$: | *PC compressive strength at 7 days [MPa]* |
| $\Delta$: | *Sample compressive strength [MPa]* |
| $\rho$: | *Slurry density [g/ cm$^3$]* |
| $\varphi$: | *volume fraction of free fluid [%]* |
| $m_S$: | *Slurry mass [g]* |
| $E$: | *Young's Modulus [MPa]* |
| $E'$: | *Material stiffness [MPa]* |
| $E''$: | *Loss modulus [MPa]* |
| $E^*$: | *Complex modulus [MPa]* |
| $T_0$: | *Initial chamber temperature [°C]* |
| $T_i$: | *Chamber temperature at time i [°C]* |
| $V_{FF}$: | *Collected volume [cm$^3$]* |
| $WL_{CH}$: | *CH weight loss [%]* |
| $W_{140}$: | *Weight burned at 140° [g]* |

## References


Abbas, G., Irawan, S., Kumar, S., Elrayah, A.A.I., 2013. Improving Oil well Cement Slurry Performance Using Hydroxypropylmethylcellulose Polymer. Adv. Mater. Res. 787, 222–227. https://doi.org/10.4028/www.scientific.net/amr.787.222

Akhlaghi, M.A., Bagherpour, R., Kalhori, H., 2020. Application of bacterial nanocellulose fibers as reinforcement in cement composites. Constr. Build. Mater. 241, 118061. https://doi.org/10.1016/j.conbuildmat.2020.118061

Al Ramadan, M., Salehi, S., Kwatia, G., Ezeakacha, C., Teodoriu, C., 2019. Experimental investigation of well integrity: Annular gas migration in cement column. J. Pet. Sci. Eng. 179, 126–135. https://doi.org/10.1016/j.petrol.2019.04.023

Alizadeh, R., Beaudoin, J.J., Raki, L., 2011. Mechanical properties of calcium silicate hydrates. Mater. Struct. Constr. 44, 13–28. https://doi.org/10.1617/s11527-010-9605-9

API Specification 10A, 2019. Specification for Cements and Materials for Well Cementing,

Twenty-Fif. ed, American Petroleum Institute. Northwest Washington, DC.

ASTM International, 1999. ASTM C109: Standard Test Method for Compressive Strength of Hydraulic Cement Mortars. Am. Soc. Test. Mater. 04, 1–6. https://doi.org/10.1520/C0109

Balea, A., Fuente, E., Blanco, A., Negro, C., 2019. Nanocelluloses: Natural-based materials for fiber- reinforced cement composites. A critical review. Polymers (Basel). 11. https://doi.org/10.3390/polym11030518

Banthia, N., Nandakumar, N., 2003. Crack growth resistance of hybrid fiber reinforced cement composites. Cem. Concr. Compos. 25, 3–9. https://doi.org/10.1016/S0958-9465(01)00043-9

Barbash, V.A., Yaschenko, O. V., Alushkin, S. V., Kondratyuk, A.S., Posudievsky, O.Y., Koshechko, V.G., 2016. The Effect of Mechanochemical Treatment of the Cellulose on Characteristics of Nanocellulose Films. Nanoscale Res. Lett. 11, 16–23. https://doi.org/10.1186/s11671-016-1632-1

Barria, J.C., Martin, C., Pique, T., Pereira, J.M., Manzanal, D., 2018. Analysis of modified cement paste in the context of CO2 geological storage. International Symposium of Energy Geotechnics. Lugar: Laussane, Pages 402-409. Publisher: Springer, Cham. Online ISBN 978-3-319-99670-7. https://doi.org/10.1007/978-3-319-99670-7.

Barria, J.C., Manzanal, Pereira, J.M., 2019. CO2 geological storage: Performance of Cement-Rock interface. XVI Pan-American Conference on Soil Mechanics and Geotechnical Engineering 17-20 November 2019. Cancun, México. DOI: 10.3233/STAL190359

Barria, J.C., Manzanal, Pereira, J.M., Ghabezloo, S., 2020a. CO2 Geological storage: Microstructure and mechanical behaviour of cement modified with biopolymers after carbonation. E3S Web Conf. Vol. 205, 2020. 2nd International Conference on Energy Geotechnics (ICEGT 2020), section: CO2 Sequestration and Deep Geothermal Energy 18 November 2020: DOI: 10.1051/e3sconf/202020502007

Barria, J.C., Pereira, J.M., Manzanal, D., 2020b. Cement with bacterial nanocellulose

cured at high temperature: mechanical performance in the context of CO2 geological storage. Geomechanics for Energy and the Environment. Under review.

Bonett, A., Pafitis, D., 1996. Getting to the root of gas migration. Oilf. Rev. 8, 36–49.

Cao, Y., Tian, N., Bahr, D., Zavattieri, P.D., Youngblood, J., Moon, R.J., Weiss, J., 2016. The influence of cellulose nanocrystals on the microstructure of cement paste. Cem. Concr. Compos. 74, 164–173. https://doi.org/10.1016/j.cemconcomp.2016.09.008

Cao, Y., Zavaterri, P., Youngblood, J., Moon, R., Weiss, J., 2015. The influence of cellulose nanocrystal additions on the performance of cement paste. Cem. Concr. Compos. 56, 73–83. https://doi.org/10.1016/j.cemconcomp.2014.11.008

Cerrutti, P., Roldán, P., García, R.M., Galvagno, M.A., Vázquez, A., Foresti, M.L., 2016. Production of bacterial nanocellulose from wine industry residues: Importance of fermentation time on pellicle characteristics. J. Appl. Polym. Sci. 133. https://doi.org/10.1002/app.43109

Charreau, H., L. Foresti, M., Vazquez, A., 2012. Nanocellulose Patents Trends: A Comprehensive Review on Patents on Cellulose Nanocrystals, Microfibrillated and Bacterial Cellulose. Recent Pat. Nanotechnol. 7, 56–80. https://doi.org/10.2174/18722105130106

de Paula, J.N., Calixto, J.M., Ladeira, L.O., Ludvig, P., Souza, T.C.C., Rocha, J.M., de Melo, A.A.V., 2014. Mechanical and rheological behavior of oil-well cement slurries produced with clinker containing carbon nanotubes. J. Pet. Sci. Eng. 122, 274–279. https://doi.org/10.1016/j.petrol.2014.07.020

De Weerdt, K., Haha, M. Ben, Le Saout, G., Kjellsen, K.O., Justnes, H., Lothenbach, B., 2011. Hydration mechanisms of ternary Portland cements containing limestone powder and fly ash. Cem. Concr. Res. 41, 279–291. https://doi.org/10.1016/j.cemconres.2010.11.014

DeJong, M.J., Ulm, F.J., 2007. The nanogranular behavior of C-S-H at elevated temperatures (up to 700 °C). Cem. Concr. Res. 37, 1–12. https://doi.org/10.1016/j.cemconres.2006.09.006

Evans, R.H., Marathe, M.S., 1968. Microcracking and stress-strain curves for concrete in tension. Matériaux Constr. 1, 61–64. https://doi.org/10.1007/BF02479001

Foray-thevenin, G., Vigier, G., Vassoille, R., Orange, G., 2006. Characterization of cement paste by dynamic mechanical Part I : operative conditions 56, 129–137. https://doi.org/10.1016/j.matchar.2005.10.007

Fu, T., Montes, F., Suraneni, P., Youngblood, J., Weiss, J., 2017. The influence of cellulose nanocrystals on the hydration and flexural strength of Portland cement pastes. Polymers (Basel). 9. https://doi.org/10.3390/polym9090424

García, C., 2012. Caracterización térmica y mecánica de polibutilentereftalato (PBT). Univ. politécnica Cart. Universidad Politécnica de Cartagena.

Gómez Hoyos, C., Cristia, E., Vázquez, A., 2013. Effect of cellulose microcrystalline particles on properties of cement based composites. Mater. Des. 51, 810–818. https://doi.org/10.1016/j.matdes.2013.04.060

Hisseine, O.A., Omran, A.F., Tagnit-Hamou, A., 2018. Influence of cellulose filaments on cement paste and concrete. J. Mater. Civ. Eng. 30, 1–14. https://doi.org/10.1061/(ASCE)MT.1943-5533.0002287

Hisseine, O.A., Wilson, W., Sorelli, L., Tolnai, B., Tagnit-Hamou, A., 2019. Nanocellulose for improved concrete performance: A macro-to-micro investigation for disclosing the effects of cellulose filaments on strength of cement systems. Constr. Build. Mater. 206, 84–96. https://doi.org/10.1016/j.conbuildmat.2019.02.042

Hoyos, C.G., Zuluaga, R., Gañán, P., Pique, T.M., Vazquez, A., 2019. Cellulose nanofibrils extracted from fique fibers as bio-based cement additive. J. Clean. Prod. 235, 1540–1548. https://doi.org/10.1016/j.jclepro.2019.06.292

Jamshidi, M., Karimi, M., 2009. Characterization of Polymeric Fibers as Reinforcements of Cement-Based Composites. J. Appl. Polym. Sci. 115, 2779–2785. https://doi.org/10.1002/app

Jawaid, M., Khalil, H.P.S.A., Hassan, A., Dungani, R., Hadiyane, A., 2015. Composites : Part B Effect of jute fibre loading on tensile and dynamic mechanical properties of oil

palm epoxy composites. Compos. Part B 45, 619–624. https://doi.org/10.1016/j.compositesb.2012.04.068

Jozala, A.F., Lencastre-novaes, L.C. De, Lopes, A.M., Santos-ebinuma, V.D.C., Mazzola, P.G., Pessoa-jr, A., 2016. Bacterial nanocellulose production and application : a 10-year overview. Appl. Microbiol. Biotechnol. 100, 2063–2072. https://doi.org/10.1007/s00253-015-7243-4

Keshk, S.M.A.S., 2014. Bacterial Cellulose Production and its Industrial Applications. J. Bioprocess. Biotech. 4. https://doi.org/10.4172/2155-9821.1000150

Kiran, R., Teodoriu, C., Dadmohammadi, Y., Nygaard, R., Wood, D., Mokhtari, M., Salehi, S., 2017. Identification and evaluation of well integrity and causes of failure of well integrity barriers (A review). J. Nat. Gas Sci. Eng. 45, 511–526. https://doi.org/10.1016/j.jngse.2017.05.009

Klemm, D., Schumann, D., Kramer, F., Heßler, N., Hornung, M., Marsch, S., Gesichtschirurgie, K.-, Chirurgie, P., Jena, F., Allee, E., V, P.J., 2006. Nanocelluloses as Innovative Polymers in Research and Application. Adv. Polym. Sci. 49–96. https://doi.org/10.1007/12_097

Lee, H.J., Kim, S.K., Lee, H.S., Kim, W., 2019. A Study on the Drying Shrinkage and Mechanical Properties of Fiber Reinforced Cement Composites Using Cellulose Nanocrystals. Int. J. Concr. Struct. Mater. 13. https://doi.org/10.1186/s40069-019-0351-2

Li, Z., Ahadi, K., Jiang, K., Ahvazi, B., Li, P., Anyia, A.O., Cadien, K., Thundat, T., 2017. Freestanding hierarchical porous carbon film derived from hybrid nanocellulose for high-power supercapacitors. Nano Res. 10, 1847–1860. https://doi.org/10.1007/s12274-017-1573-8

Liu, L., Ha, J., Hashida, T., Teramura, S., 2001. Development of a CO2solidification method for recycling autoclaved lightweight concrete waste. J. Mater. Sci. Lett. 20, 1791–1794. https://doi.org/10.1023/A:1012591318077

Ma, B., Ou, Z., Jian, S., Xu, R., 2011. Influence of cellulose ethers on hydration products

of portland cement. J. Wuhan Univ. Technol. Mater. Sci. Ed. 26, 588–593. https://doi.org/10.1007/s11595-011-0273-6

Marsh, B.K., Day, R.L., 1988. Pozzolanic and cementitious reaction of fly ash in blended. Cem. Concr. Res. 18, 301–310. https://doi.org/https://doi.org/10.1016/0008-8846(88)90014-2

Mejdoub, R., Hammi, H., Suñol, J.J., Khitouni, M., Boufi, S., 2017. Nanofibrillated cellulose as nanoreinforcement in Portland cement : Thermal , mechanical and microstructural properties. J. Compos. Mater. 51, 2491–2503. https://doi.org/10.1177/0021998316672090

Mikkelsen, D., Flanagan, B.M., Dykes, G.A., Gidley, M.J., 2009. Influence of different carbon sources on bacterial cellulose production by Gluconacetobacter xylinus strain ATCC 53524. J. Appl. Microbiol. 107, 576–583. https://doi.org/10.1111/j.1365-2672.2009.04226.x

Mohammadkazemi, F., Aguiar, R., Cordeiro, N., 2017. Improvement of bagasse fiber–cement composites by addition of bacterial nanocellulose: an inverse gas chromatography study. Cellulose 24, 1803–1814. https://doi.org/10.1007/s10570-017-1210-4

Mohammadkazemi, F., Doosthoseini, K., Ganjian, E., Azin, M., 2015. Manufacturing of bacterial nano-cellulose reinforced fiber-cement composites. Constr. Build. Mater. 101, 958–964. https://doi.org/10.1016/j.conbuildmat.2015.10.093

Moumin, M., Plank, J., 2017. Effectiveness of Polycarboxylate Dispersants in Enhancing the Fluid Loss Performance of Cellulose Ethers. SPE Int. Conf. Oilf. Chem. https://doi.org/10.2118/184542-ms

Muhd Julkapli, N., Bagheri, S., 2017. Nanocellulose as a green and sustainable emerging material in energy applications: a review. Polym. Adv. Technol. 28, 1583–1594. https://doi.org/10.1002/pat.4074

Nelson, E.B., 1990. Well Cementing. Elsevier.

Palou, M.T., Šoukal, F., Boháč, M., Šiler, P., Ifka, T., Živica, V., 2014. Performance of G-

Oil Well cement exposed to elevated hydrothermal curing conditions. J. Therm. Anal. Calorim. 118, 865–874. https://doi.org/10.1007/s10973-014-3917-x

Pane, I., Hansen, W., 2005. Investigation of blended cement hydration by isothermal calorimetry and thermal analysis. Cem. Concr. Res. 35, 1155–1164. https://doi.org/10.1016/j.cemconres.2004.10.027

Parveen, S., Rana, S., Fangueiro, R., Conceiç, M., 2017. A novel approach of developing micro crystalline cellulose reinforced cementitious composites with enhanced microstructure and mechanical performance. Cem. Concr. Compos. 78. https://doi.org/10.1016/j.cemconcomp.2017.01.004

Pourbeik, P., Alizadeh, R., Beaudoin, J.J., Nguyen, D.T., Raki, L., 2013. Microindentation creep of 45 year old hydrated Portland cement paste. Adv. Cem. Res. 25, 301–306. https://doi.org/10.1680/adcr.12.00058

Puertas, F., Santos, H., Palacios, M., Mart&#65533;nez-Ram&#65533;rez, S., 2005. Polycarboxylate superplasticiser admixtures: effect on hydration, microstructure and rheological behaviour in cement pastes. Adv. Cem. Res. 17, 77–89. https://doi.org/10.1680/adcr.17.2.77.65044

Ramasamy, J., Amanullah, M., 2020. Nanocellulose for oil and gas field drilling and cementing applications. J. Pet. Sci. Eng. 184. https://doi.org/10.1016/j.petrol.2019.106292

Saba, N., Tahir, P.M., 2016. A Review on Dynamic mechanical analysis of natural fibre reinforced polymer composites. Constr. Build. Mater. 106, 149–159. https://doi.org/10.1016/j.conbuildmat.2015.12.075

Salehi, S., Khattak, M., Ali, N., Rizvi, H., 2016. Laboratory Investigation of High Performance Geopolymer Based Slurries AADE-16-FTCE-88. Am. Assoc. Drill. Eng.

Savastano, H., Warden, P.G., Coutts, R.S.P., 2005. Microstructure and mechanical properties of waste fibre-cement composites, in: Cement and Concrete Composites. pp. 583–592. https://doi.org/10.1016/j.cemconcomp.2004.09.009

Sereda, P.J., Feldman, R.F., Swenson, E.G., 1966. Effect of sorbed water on some

mechanical properties of hydrated Portland cement pastes and compacts. Highw. Res. Board … 58–73.

Sheykhnazari, S., Tabarsa, T., Ashori, A., Shakeri, A., Golalipour, M., 2011. Bacterial synthesized cellulose nanofibers; Effects of growth times and culture mediums on the structural characteristics. Carbohydr. Polym. 86, 1187–1191. https://doi.org/10.1016/j.carbpol.2011.06.011

Sun, X., Wu, Q., Lee, S., Qing, Y., Wu, Y., 2016. Cellulose Nanofibers as a Modifier for Rheology, Curing and Mechanical Performance of Oil Well Cement. Sci. Rep. 6, 1–9. https://doi.org/10.1038/srep31654

Sun, X., Wu, Q., Zhang, J., Qing, Y., Wu, Y., Lee, S., 2017. Rheology, curing temperature and mechanical performance of oil well cement: Combined effect of cellulose nanofibers and graphene nano-platelets. Mater. Des. 114, 92–101. https://doi.org/10.1016/j.matdes.2016.10.050

Tuutti, K., 1982. Corrosion of Steel in Concrete. Swedish Cem. Concr. Res. Inst. 469. https://doi.org/10.1002/9780470872864.ch49

Vazquez, A., Foresti, M.L., Cerrutti, P., Galvagno, M., 2013. Bacterial Cellulose from Simple and Low Cost Production Media by Gluconacetobacter xylinus. J. Polym. Environ. 21, 545–554. https://doi.org/10.1007/s10924-012-0541-3

Vázquez, A., Pique, T.M., 2017. Biobased Additives in Oilwell Cement, in: Industrial Applications of Renewable Biomass Products. Past, Present and Future. pp. 179–198. https://doi.org/10.1007/978-3-319-61288-1

Wild, S., Khatib, J.M., 1997. Portlandite consumption in metakaolin cemen pastes and mortars. Cem. Concr. Res. 27, 137–146. https://doi.org/https://doi.org/10.1016/S0008-8846(96)00187-1

Xiaofeng, C., Shanglong, G., Darwin, D., McCabe, S.L., 1990. Role of silica fume in compressive strength of cement paste, mortar, and concrete. ACI Mater. J. 89, 375–387. https://doi.org/10.14359/2570

## Table captions

Table 1. Cement chemical composition.

Table 2. Bacterial nanocellulose content in cement paste.

Table 3. Consistometry test.

Table 4. CH content and DOH (%) of the samples.

Table 5. BNC and SP percentages in cement samples.

## Figure captions

Figure 1. Bacteria and bacterial nanocellulose (Courtesy of Cerruti et al. 2016)

Figure 2. Ultrasonic bath for homogenization of BNC - distilled water mixture.

Figure 3. Compressive strength test equipment.

Figure 4. Testing methodology.

Figure 5. Free fluid content for different percentages of superplasticizer for Portland Cement (PC) and PC + 0.05% BNC.

Figure 6. Consistometry test for Portland Cement (PC), PC + 0.05% of BNC + 0.35% SP and PC + 0.05% BNC + 0.40% SP.

Figure 7. (a) Example of mass loss calculation for CH in the TGA test (b)TGA results for Portland Cement (PC) and PC modified with BNC at 0.05%, 0.10%, 0.15% and 0.20% BWOC.

Figure 8. DrTGA results for Portland Cement (PC) and PC modified with BNC at 0.05%, 0.10%, 0.15% and 0.20% BWOC.

Figure 9. DMA results of Portland Cement (PC) and PC modified with BNC at 0.05%, 0.10%, 0.15% and 0.20% BWOC samples cured for 28 days.

Figure 10. Normalized storage modulus of Portland Cement (PC) and PC modified with BNC at 0.05%, 0.10%, 0.15% and 0.20% BWOC samples cured for 28 days.

Figure 11 DMA results in term of tan d of Portland Cement (PC) and PC modified with BNC at 0.05%, 0.10%, 0.15% and 0.20% BWOC samples cured for 28 days.

Figure 12. Normalized compressive strength of Portland Cement (PC) and PC modified with BNC at 0.05%, 0.10%, 0.15% and 0.20% BWOC samples cured for 7 and 28 days as a function of the percentage of nanocellulose: Diamonds symbols represent samples cured for 7 days and squares symbols represent samples with 28 days of curing. The values have been normalized to the strength value obtained after 7 days of curing in PC cement.

Figure 13. Unconfined Compressive Strength for of Portland Cement (PC) and PC modified with BNC at 0.05%, 0.10%, 0.15% and 0.20% BWOC samples at three curing times: 8h, 7 days and 28 days.

**Table 1**. Cement chemical composition.

| Composition | CaO | $SiO_2$ | MgO | $Al_2O_3$ | $Fe_2O_3$ | $SO_3$ | Total alkalieq |
|---|---|---|---|---|---|---|---|
| (wt%) | 62.39 | 21.23 | 2.22 | 3.84 | 5.07 | 2.40 | 0.64 |

**Table 2**. Bacterial nanocellulose content in cement paste.

| Mix | Additive [g] | BNC [g] | Added Water[g] | Water [g] | Total water [g] | Cement [g] | BNC content [%] |
|---|---|---|---|---|---|---|---|
| 1 | 0 | 0 | 0 | 349 | 349 | 792 | 0.00 |
| 2 | 86.09 | 0.40 | 85.69 | 263.31 | 349 | 792 | 0.05 |
| 3 | 172.17 | 0.79 | 171.38 | 177.62 | 349 | 792 | 0.10 |
| 4 | 258.26 | 1.19 | 257.07 | 91.93 | 349 | 792 | 0.15 |
| 5 | 342.80 | 1.58 | 341.22 | 7.78 | 349 | 792 | 0.20 |

**Table 3**. Consistometry test.

| Test | BNC [%] | SP [%] | Initial consistency [Bearden] | Thickening time [min] |
|---|---|---|---|---|
| 1 | 0 | 0 | 15 | 99 |
| 2 | | 0.05 | Excessively viscous | - |
| 3 | | 0.15 | Excessively viscous | - |
| 4 | 0.05 | 0.3 | Excessively viscous | - |
| 5 | | 0.35 | 35 | 99 |
| 6 | | 0.4 | 12 | 126 |

**Table 4**. CH content and DOH (%) of the samples.

| Sample | BNC [%] | CH [%] | DOH [%] |
|---|---|---|---|
| 1 | 0 | 19.92% | 62.96 |
| 2 | 0.05 | 22.16% | 66.13 |
| 3 | 0.1 | 22.45% | 64.62 |
| 4 | 0.15 | 22.67% | 68.34 |
| 5 | 0.2 | 22.58% | 66.88 |

**Table 5**. BNC and SP percentages in cement samples.

| Sample | | Cement [g] | Water [g] | Curing [days] | BNC [% BWOC] | SP [% BWOC] |
|---|---|---|---|---|---|---|
| 1 | - | 792 | 349 | 7 | 0 | 0 |
| 2 | - | 792 | 349 | 7 | 0.05 | 0.4 |
| 3 | - | 792 | 349 | 7 | 0.10 | 0.4 |

| | | | | | | |
|---|---|---|---|---|---|---|
| 4 | - | 792 | 349 | 7 | 0.15 | 0.55 |
| 5 | - | 792 | 349 | 7 | 0.20 | 0.7 |
| - | 1 | 792 | 349 | 28 | 0 | 0 |
| - | 2 | 792 | 349 | 28 | 0.05 | 0.35 |
| - | 3 | 792 | 349 | 28 | 0.10 | 0.35 |
| - | 4 | 792 | 349 | 28 | 0.15 | 0.5 |
| - | 5 | 792 | 349 | 28 | 0.20 | 0.6 |

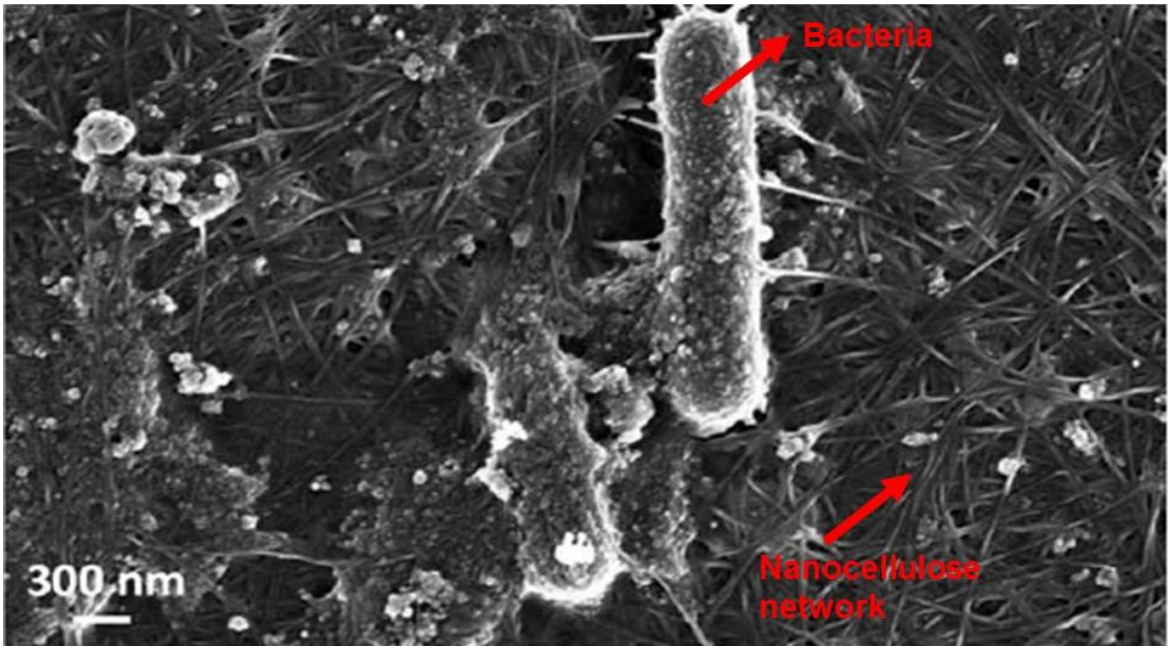



Figure 1. Bacteria and bacterial nanocellulose (Courtesy of Cerruti et al. 2016)




Figure 2. Ultrasonic bath for homogenization of BNC - distilled water mixture.



Figure 3. Compressive strength test equipment.

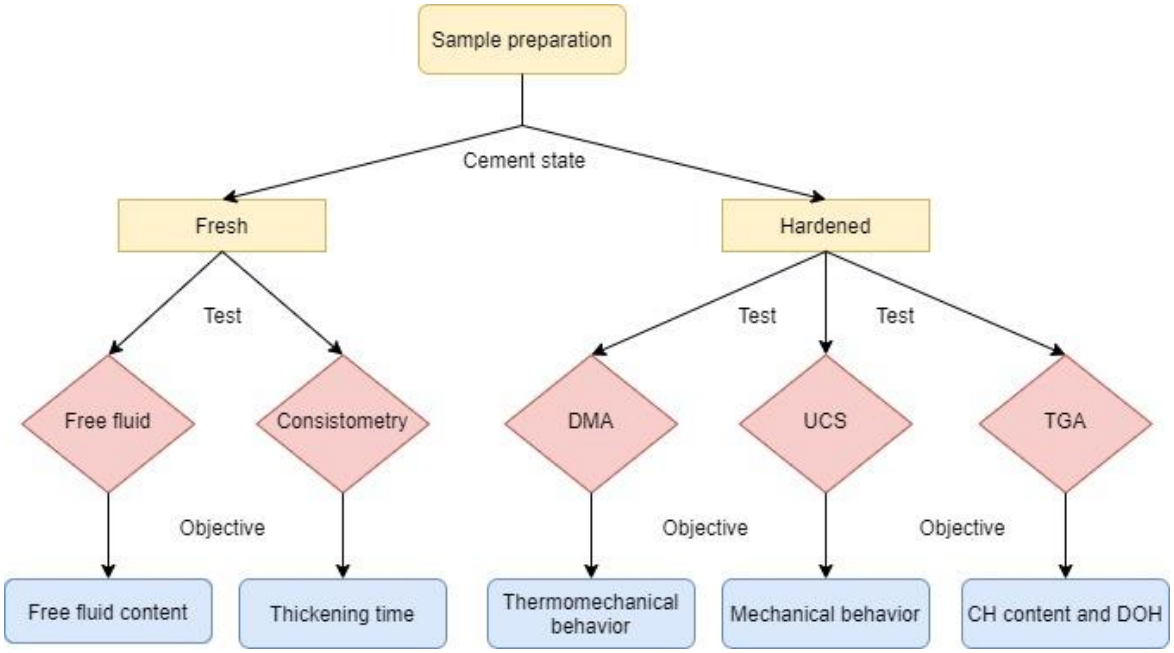



Figure 4. Testing methodology.

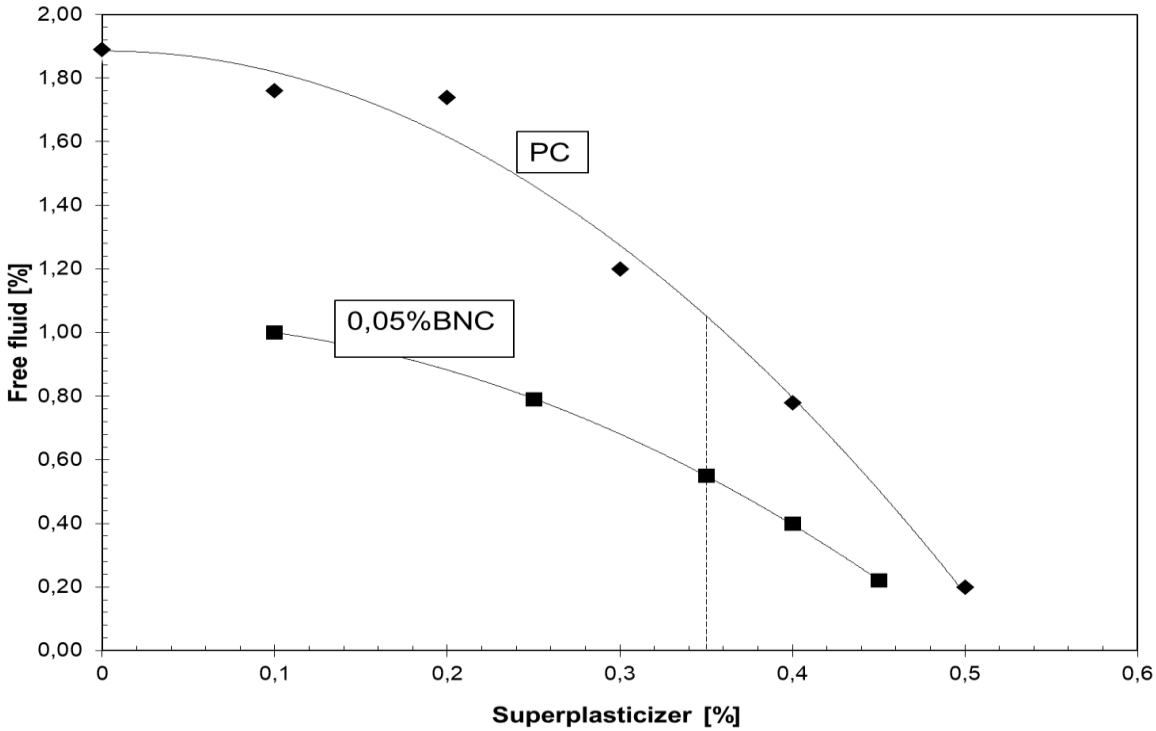



Figure 5. Free fluid content for different percentages of superplasticizer for Portland Cement (PC) and PC + 0.05% BNC.

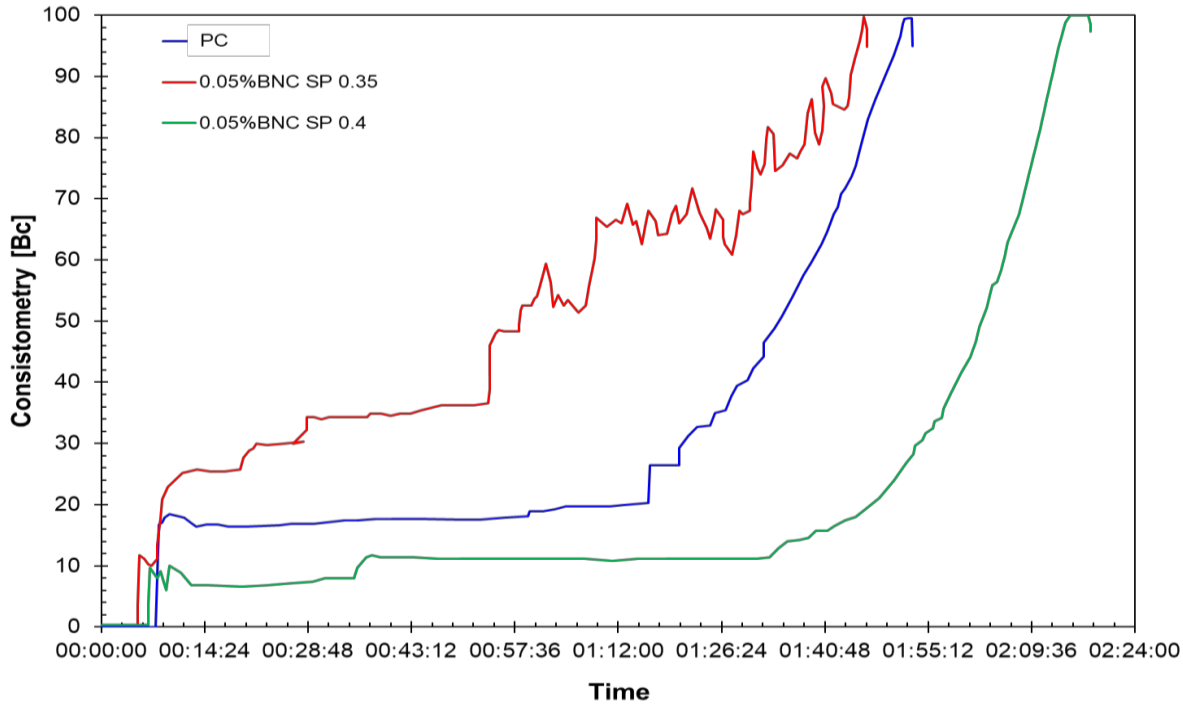



Figure 6. Consistometry test for Portland Cement (PC), PC + 0.05% of BNC + 0.35% SP and PC + 0.05% BNC + 0.40% SP.

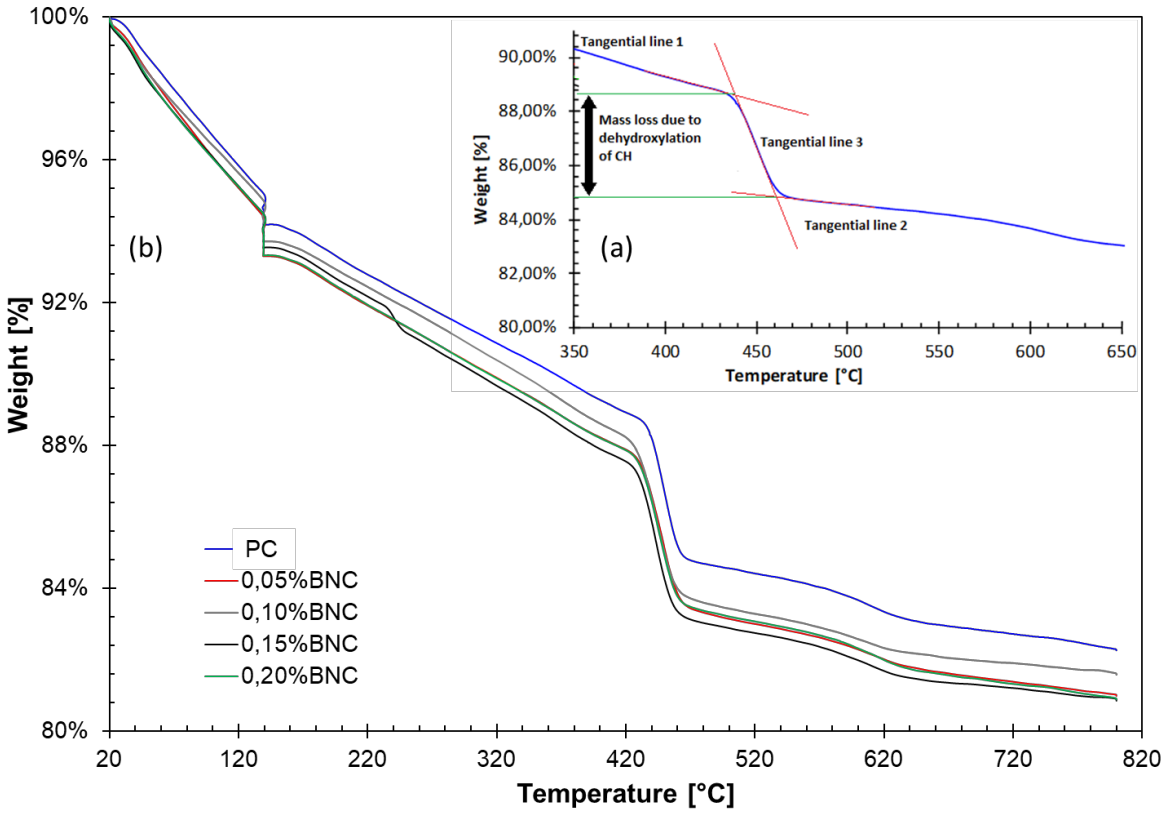



Figure 7. (a) Example of mass loss calculation for CH in the TGA test (b)TGA results for Portland Cement (PC) and PC modified with BNC at 0.05%, 0.10%, 0.15% and 0.20% BWOC.

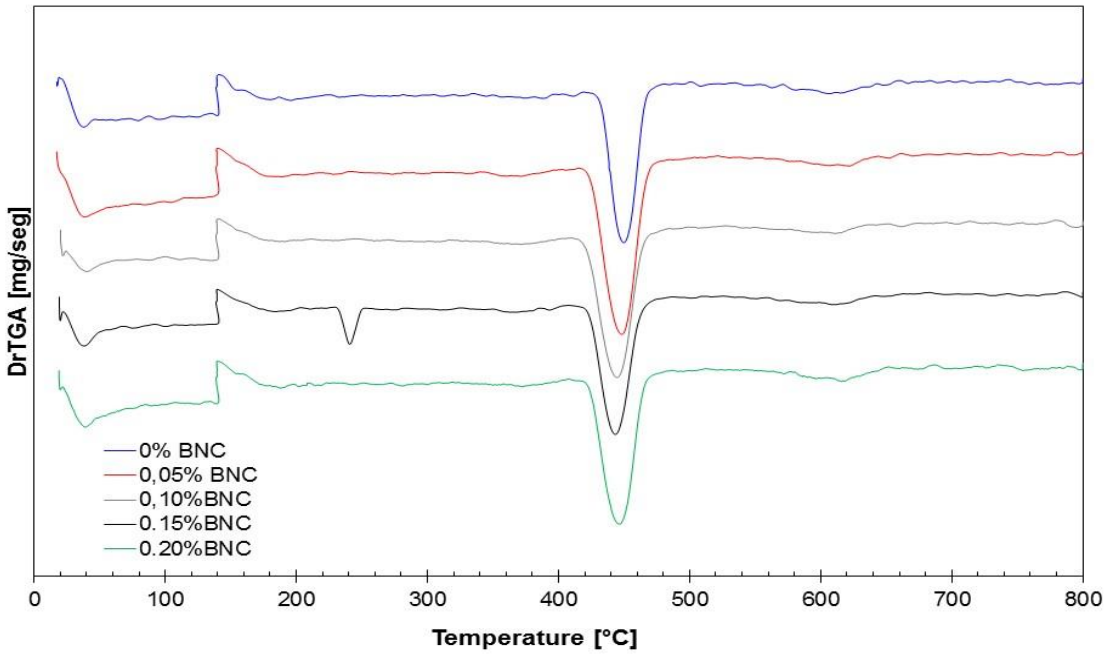



Figure 8. DrTGA results for Portland Cement (PC) and PC modified with BNC at 0.05%, 0.10%, 0.15% and 0.20% BWOC.

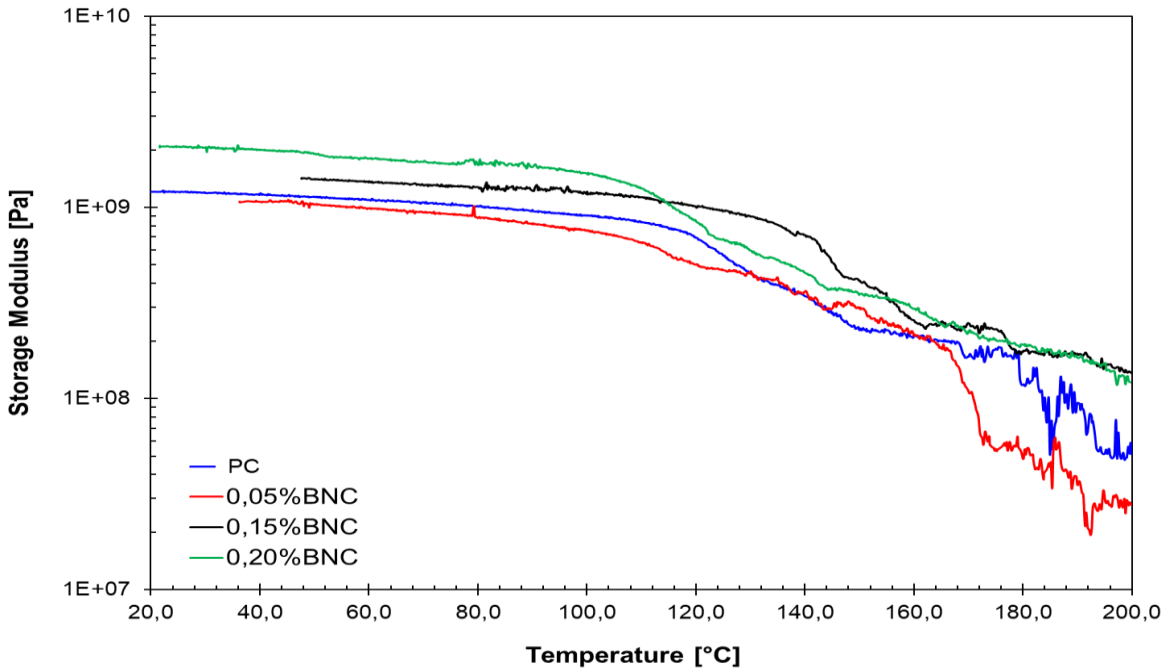



Figure 9. DMA results of Portland Cement (PC) and PC modified with BNC at 0.05%, 0.10%, 0.15% and 0.20% BWOC samples cured for 28 days.

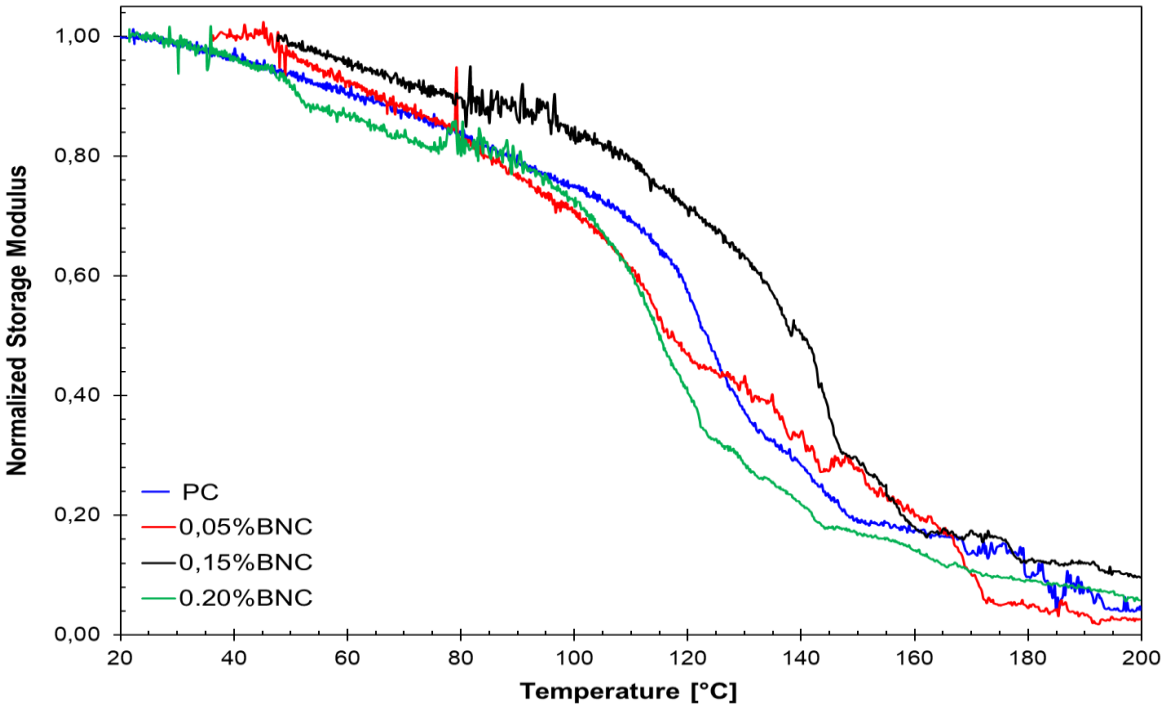



Figure 10. Normalized storage modulus of Portland Cement (PC) and PC modified with BNC at 0.05%, 0.10%, 0.15% and 0.20% BWOC samples cured for 28 days.

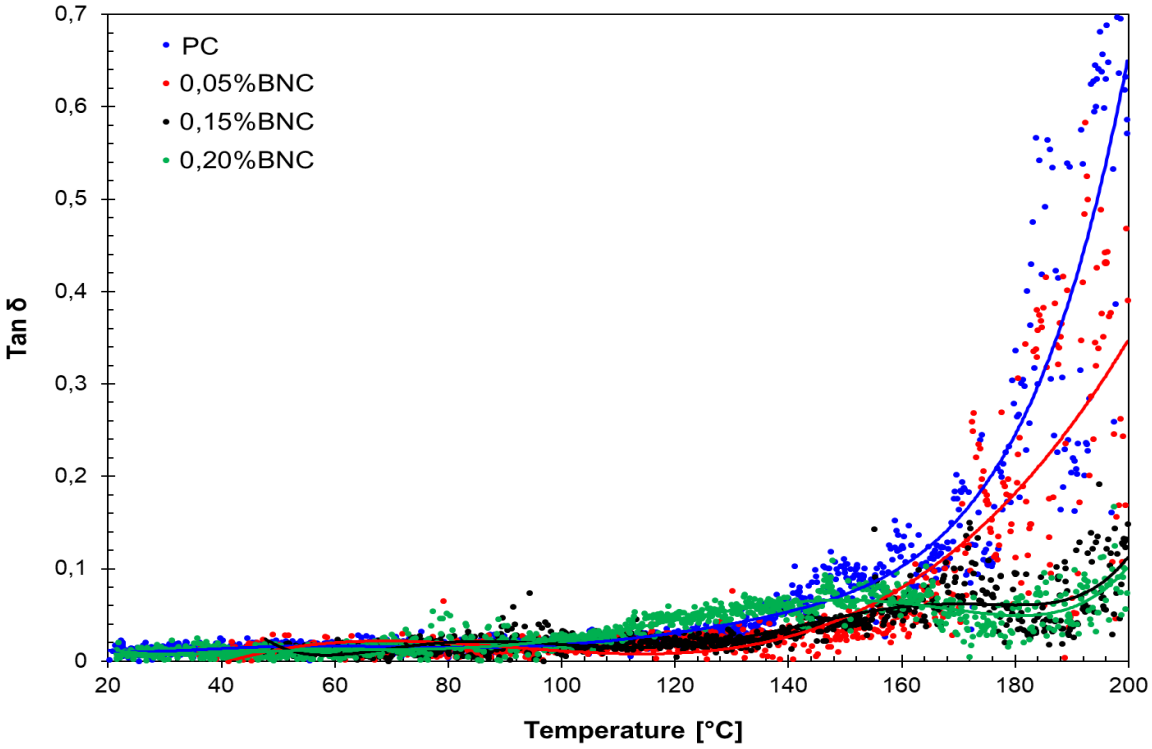



Figure 11. DMA results in term of tan δ of Portland Cement (PC) and PC modified with BNC at 0.05%, 0.10%, 0.15% and 0.20% BWOC samples cured for 28 days.

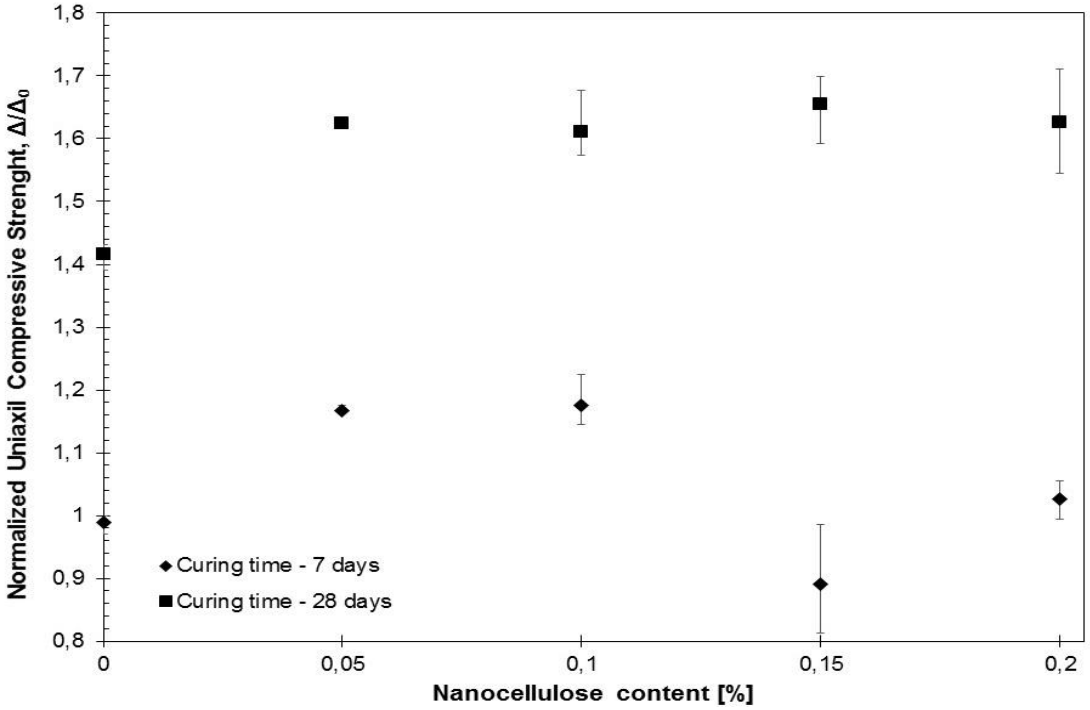



Figure 12. Normalized compressive strength of Portland Cement (PC) and PC modified with BNC at 0.05%, 0.10%, 0.15% and 0.20% BWOC samples cured for 7 and 28 days as a function of the percentage of nanocellulose: Diamonds symbols represent samples cured for 7 days and squares symbols represent samples with 28 days of curing. The values have been normalized to the strength value obtained after 7 days of curing in PC cement.

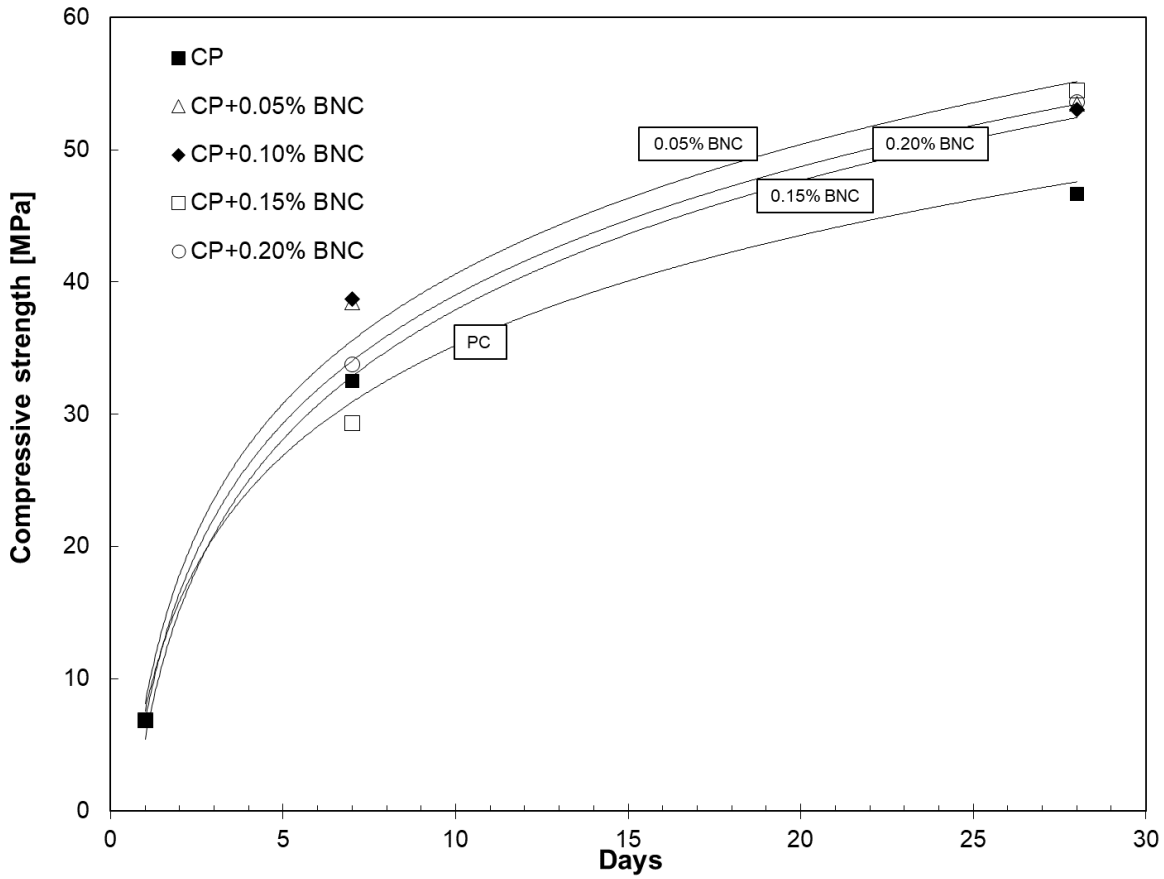



Figure 13. Unconfined Compressive Strength for of Portland Cement (PC) and PC modified with BNC at 0.05%, 0.10%, 0.15% and 0.20% BWOC samples at three curing times: 8h, 7 days, and 28 days. Only the average values of the results were considered.

# Highlights

Incorporation of bacteria nano cellulose in oil-well cement improves the strength of hardened samples.

Thermogravimetric analysis shows an increment in hydration products and hydration degree with bacterial nanocellulose

Enhancement of thermal stability and tensile reinforcement has been observed using large percentages of bacterial nanocellulose.